

BlockFLEX: An Adaptive and Survivable Architecture with Hierarchical Routing for LEO Satellite Networks

Xiangtong Wang
Sichuan University

Abstract

This paper presents **BlockFLEX**, an adaptive and survivable architecture with a hierarchical routing scheme for Low Earth Orbit satellite networks, designed to address dynamic topology changes and severe link failures. By organizing satellites into autonomous blocks, BlockFLEX establishes a survivable underlay network that masks network volatility and offers a stable overlay view. The architecture employs a hierarchical routing scheme integrating both convergence-free geographic routing and convergence-isolated routing. Furthermore, BlockFLEX adaptively switches between stateful and stateless forwarding modes, enabling efficient, resilient, and stable routing via a dedicated protection mechanism and an optimized source satellite selection algorithm.

Experimental evaluations on current operational LEO satellite networks (LSNs) demonstrate that under scenarios with up to 30% random link failures, the proposed method achieves a $2\times$ improvement in reachability compared to current leading schemes, while maintaining near-100% routing availability. Moreover, the overhead of control messages and forwarding information base (FIB) updates remains below 0.2% of that in OSPF, accompanied by a $\geq 36\%$ reduction in routing computation time and a $\geq 50\%$ decrease in latency jitter.

1 Introduction

In recent years, low Earth orbit satellite networks (LSNs) have emerged as a promising complementary infrastructure to terrestrial networks, offering ubiquitous Internet connectivity to approximately 2.7 billion unserved users in remote regions, developing nations, aviation, and maritime environments [21]. Unlike traditional Geostationary Earth Orbit (GEO) satellite networks [9, 58], LEO mega-constellations leverage densely deployed satellites with inter-satellite links (ISLs) to provide low-latency, full-coverage, and high-bandwidth services. Recent commercial ventures have demonstrated the feasibility of large-scale LSNs [2, 6, 13, 50], reshaping global connectivity paradigms.

Despite the significant promise of LSNs, LSNs introduce unique challenges for routing design due to distinctive orbital dynamics. LEO satellites move at orbital velocities around 7.6 km/s relative to Earth [42, 51], resulting in highly dynamic satellite-ground interactions that fundamentally differ from terrestrial or GEO satellite networks. Furthermore, inter-satellite links (ISLs) are susceptible to disruptions from sun outage, orbital maneuvers, and relative motion, leading to intermittent failures [24, 42]. These dynamics and failures

contribute to persistent network volatility, complicating the maintenance of a stable underlay and feasible routing.

Existing approaches attempt to address these issues through orbit-prediction-based routing [43, 56], satellite-ID addressing [7, 8, 25, 29], or geographic routing under convergence-free policies [29, 33, 35, 41]. However, these methods struggle to simultaneously achieve survivability, efficiency, and resiliency at scale, all of which are essential qualities for supporting future mass user access.

We observe that the volatility in LSNs exhibits distributed characteristics and can be localized and individually mitigated to enhance the underlay network survivability [8, 28, 33] while minimizing their cascading effects on routing performance. Moreover, purely stateless forwarding fails to balance efficiency and resilience [32, 52], whereas stateful approaches often lack adaptability in highly dynamic conditions. The core challenge is therefore to enable resilient, efficient, and stable routing over a survivable underlay. To this end, we propose BlockFlex, an adaptive and survivable architecture featuring hierarchical routing for LSNs. Its key components include:

- 1) A **Dynamic Adaptive Block Network (DABNet)**, which partitions the satellite network into autonomous domains (blocks) to isolate volatility from intermittent ISL failures and provides a stable network view for routing (§4).
- 2) A hierarchical routing scheme, **DABR**, operating over DABNet. It employs a divide-and-conquer strategy to confine convergence scope while maintaining global convergence-free routing policy (§5).

We evaluate the BlockFlex with the currently operational LSNs on an open-source testbed to implement our prototype. Under scenarios with up to 30% unpredictable intermittent ISL failures, BlockFlex achieves a $2\times$ improvement in packet delivery ratio over state-of-the-art schemes while maintaining near-100% routing reachability. Notably, the control message and forwarding information base (FIB) update overhead is below 0.2% of convergent routing protocols such as OSPF [12], with additional improvements including $\geq 36\%$ reduction in time consumption of routing computation and $\geq 50\%$ reduction in latency jitter.

Summary. The main contributions of this work, supported by the BlockFLEX prototype, are summarized as follows:

◆ **Distributed LSN volatility masking.** We design and implement the distributed underlay network for LSNs that effectively masks the impact of intermittent link failures on routing. This approach maintains network survivability even under severe failure conditions.

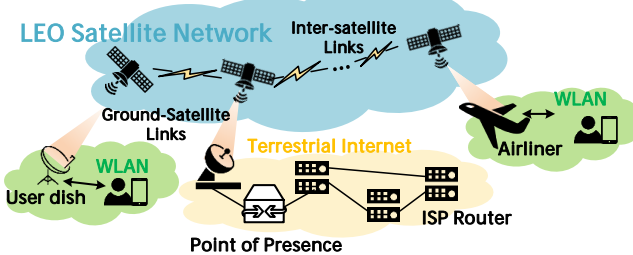


Figure 1: Today’s LEO satellite network architecture.

- ♦ **Resilient and efficient LSN routing.** By combining the advantages of both convergence-free and convergence-isolated routing paradigms, along with a distributed resilience strategy and hybrid stateful-stateless forwarding, we achieve for the first time a routing scheme that simultaneously ensures both efficiency and resilience with fully distributed manner.
- ♦ **Terrestrial-Interoperable addressing architecture.** We introduce a novel hierarchical addressing framework that ensures seamless interoperability with existing terrestrial network protocols.

2 Background

2.1 LEO satellite network architecture.

Fig. 1 illustrates the architecture of LEO satellite networks, comprising space, ground, and user segments. The space segment consisting of thousands of LEO satellites, the ground segment consisting of an operational terrestrial network with ground stations, and the user segment consisting of user dishes, terminals and airlines. The space segment enables global connectivity via high-speed inter-satellite links (ISLs). User terminals first transmit data through multi-hop ISLs [48, 51, 59], then to a ground station (GS) via a ground-to-satellite link (GSL). The data subsequently traverses a Point-of-Presence (PoP), where carrier-grade NAT performs IP address translation before reaching terrestrial servers. Terminal users access the Internet through an LSN, with packets initially uplinked to a satellite and then downlinked via a GSL. If the serving satellite lacks direct GS connectivity, the data is relayed through multiple ISL hops until reaching a satellite with GSL access.

2.2 The Considerations in LSN Design

Since most LSNs are still under intensive development, making well-informed design choices in advance is critical for satellite Internet operators. From a network design perspective, we generalize three fundamental requirements for future LSNs:

Survivability. Network survivability generally refers to the ability of a network to maintain acceptable service levels dur-

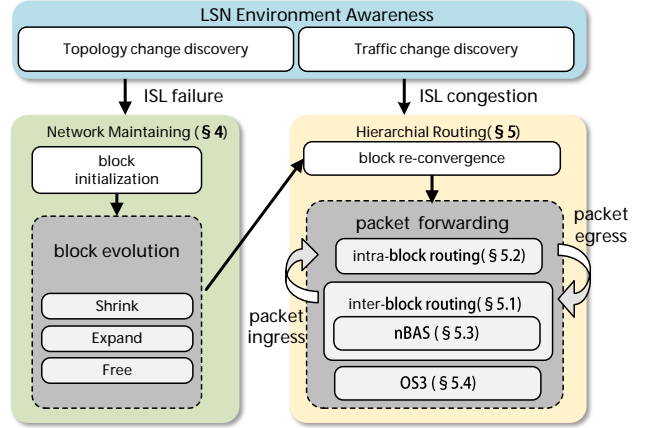


Figure 2: The BlockFLEX workflow.

ing various failure scenarios. In LSNs, space routers operate under highly complex and volatile space conditions, making them susceptible to multiple forms of interference and potential failures. Furthermore, LEO broadband constellations predominantly rely on small satellites, which have relatively short operational lifespans and higher inherent failure rates. Thus, it is essential for LSNs to exhibit strong survivability to ensure continuous operation in challenging orbital environments.

Availability. As a large-scale infrastructure requiring substantial investment, LSNs achieve economic viability by serving massive user populations, as demonstrated by Starlink’s reported profitability in 2021 and its over 5.4 million subscribers by March 2025 [38, 47]. To sustainably support such scale, these networks must maintain high service availability while ensuring routing efficiency and minimizing operational overhead.

Scalability. The evolution of LSNs is characterized by continuous deployment. The infrastructure and user base are expected to grow over time, while satellite decommissioning and replenishment remain ongoing processes. Hence, scalability constitutes a core system requirement. On one hand, the system should support “hot-swap” deployment capabilities to allow seamless incremental expansion. On the other hand, as the infrastructure scales, system availability must improve correspondingly to sustain performance under growing user demand.

3 System Design and Overview

Core ideas. To address performance issues caused by the volatility of LSN, our proposed BlockFlex comprises two core ideas. First, we abstract a **Dynamic Adaptive Block Network (DABNet)** over the conventional LSN architecture. This architecture organizes multiple neighboring satellites into autonomous domains, termed **blocks**, to mitigate the in-

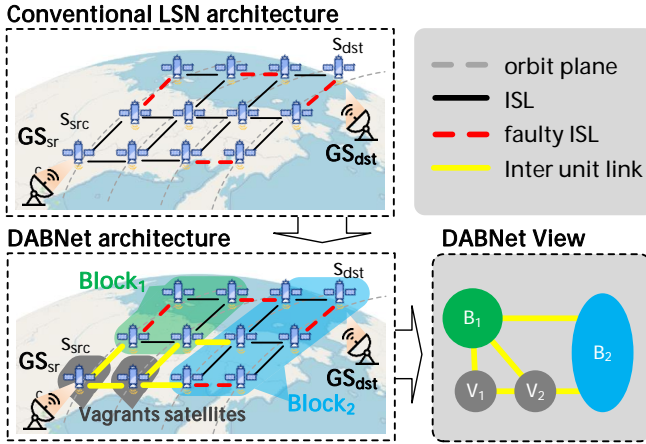


Figure 3: The DABNet architecture and view.

herent volatility of the entire LSN. Each block maintains a localized and concentrated control plane, thereby avoiding excessive control traffic overhead. From a DABNet-level view, this abstraction improves adjacency with neighboring blocks through increased external connectivity while enhancing fault tolerance via redundant Inter-unit links. Second, we propose a hierarchical routing scheme (**DABR**) over DABNet. This scheme leverages the adaptive properties of DABNet to establish a two-level routing hierarchy, comprising intra-block routing (within a single block) and inter-block routing (across multiple blocks). By employing convergence-free geographical routing between blocks and convergence-isolated routing within blocks, DABR effectively reduces route recomputation overhead caused by ISL failures or congestion while maintaining high network resilience. Fig.2 plots the workflow illustrating how BlockFlex cope with the network failure and the traffic dynamics, mainly includes 2 phases: survivable network maintaining and hierarchy routing.

- **Underlay network maintaining (§4).** Given an initial network, it will evolve into blocks as a single node needs to evolve. When the state of a satellite or link changes, e.g., failure, congestion, blocks adjacent to the satellite may need to be re-evolved.
- **overlay network routing (§5).** After each block evolves, each block has to perform the corresponding route re-convergence to maintain the consistency of information within the block, thus completing packet forwarding.

4 Dynamic Adaptive Block Network

We introduce **Dynamic Adaptive Block Network (DABNet)** over the ordinary LSN to mask the LSN volatility and present a stable view for overlay. As the underlay of routing, DABNet’s survivability refers to the ability to maintain a stable topology view in the face of volatile LSNs, thereby providing

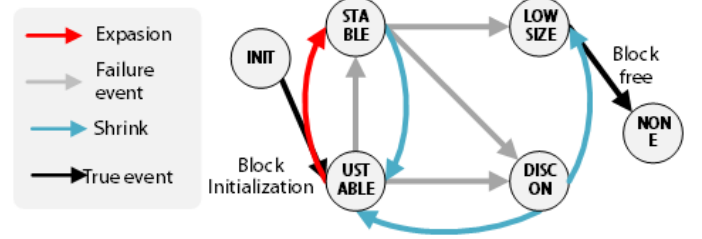


Figure 4: Block state transition diagram.

Satellite Status		
Status	Abbr.	Description
vagrant	VAGRANT	Not belonging to any block
assigned	ASSIGNED	Assigned to a specific block
fault	FAULT	Node failure, all links unavailable
Block Status		
Status	Abbr.	Description
low size	LOWSIZE	Node count or diameter below limit
disconnected	DISCONN	Block is disconnected
unstable	USTABLE	Exceeds size limit or can expand
stable	STABLE	Cannot expand (max size or no neighbors)

Table 1: Status Definitions of Forwarding Units

a foundation for stable routing in the **BlockFLEX**’s overlay network. As shown in Fig.3, we decompose the LSN into a network of multiple blocks and vagrant satellites. Each block constitutes an autonomous domain formed by multiple satellites, while vagrant satellites are those not assigned to any block. All these entities function as the forwarding units (FUs) and are connected by inter-unit links (IULs).

Based on this abstraction, it is possible to achieve (1) intrinsic fault tolerance, where intra-block ISL failures remain transparent to DABNet’s global view, and (2) significantly enhanced connectivity among forwarding units, since blocks maintain more inter-satellite links than individual satellites. This architecture substantially improves the overall survivability of the network in the presence of link failures.

4.1 DABNet Maintaining Mechanism

The maintenance of DABNet is independent of the constellation configuration in LSN, but is affected by the network environment, including failures and congestion. As the state of the network changes, each block will evolve dynamically

and adaptively to its optimal configuration. Before going further into the evolution process of block, we first define the 3 states of the satellites and 4 states of blocks involved in the DABNet, which is shown in Tab.1. The block evolution process operates based on these satellite states, progressing through the following lifecycle actions.

Block center initialization. In the initialization process, all satellites are assigned as VAGRANT state, and there will be a certain probability to become block center, at which time the state changes to ASSIGNED.

Block expansion. Block will periodically detect whether the neighboring satellite is in the VAGRANT state. If the neighboring node is in the vagrant state, block will decide whether to merge with it according to the evolution algorithm.

Block shrink. When there is an element failure in the network, e.g., node failure, link failure, the block may perform a shrink operation.

Block free. When the size or diameter of the block is smaller than the limitation and cannot be expanded any further, all contained satellites are released, at which point all satellites transition to the vagrants state. The states transition in lifecycle actions of block is shown in Fig.4. The complete maintenance framework of DABNet is detailed in Appendix.A.

4.2 Survivable LSN Partitioning

DABNet model over LSN. The LSN is modeled as a graph $\mathcal{G} = (\mathcal{S}, \mathcal{E})$, where $\mathcal{S} = \{s_1, s_2, \dots, s_{N_s}\}$ denote the set of satellites and $\mathcal{E} = \{e_1, e_2, \dots, e_{N_E}\}$ denote the set of ISLs. Then, the whole LSN can be represent by the combination of blocks, vagrants satellites and faulty satellites as:

$$\mathcal{G} = \left(\bigcup_{k=1}^{N_B} \mathcal{B}_k \bigcup \mathcal{S}_v \bigcup \mathcal{S}_f, \mathcal{E}_{IUL} \right) \quad (1)$$

where \mathcal{B}_k presents the block, i.e, the subgraph of LSN \mathcal{G} , \mathcal{S}_v are vagrant satellites, \mathcal{S}_f are fault satellites and \mathcal{E}_{IUL} are inter-unit links (the subset of ISL \mathcal{E}). Based on the basic framework of maintaining DABNet, an important research question is raised in the block evolution process: how should blocks evolve to maximize the survivability of DABNet so that it can still provide the overlay network a stable and robust topology view when faced with severe failures?

Problem Formulation. An ideal DABNet requires its blocks to exhibit sufficient internal connectivity to withstand intermittent ISL failures, while also maintaining adequate and well-distributed connections to neighboring forwarding units (blocks or vagrant satellites). This inspires us to model it as a balanced graph partitioning problem with constraints on the number of cut edges [1]. However, traditional partitioning methods present two issues:

- 1) A naive maximization of cut edges (i.e., the Inter-Unit Links) count may lead to sparse intra-block connectivity, making blocks vulnerable to internal failures.

- 2) More critically, even a high number of IULs does not guarantee robust external connectivity if these links are directionally concentrated. For instance, if all IULs of a block are clustered in one direction, packet forwarding to other directions would fail despite the high IUL count.

To address the first issue, we ensure sufficient internal connectivity by constraining the block volume, defined as the sum of the degrees of all nodes within the block. For the second issue, we introduce a novel metric, **directional connectivity** (div), to explicitly quantify the distribution uniformity of IULs around a block. Instead of merely counting IULs, we leverage the spatial characteristic of IULs and model them as vectors, computing the resultant vector magnitude. A lower magnitude indicates a more balanced directional distribution. Therefore, we formulate the **Survivable LSN Partitioning (SLP)** problem. Our objective is to maximize a compound metric $\psi(\mathcal{B}_k)$ for each block that simultaneously rewards high internal connectivity and penalizes concentrated external connectivity:

Objective

$$\max \sum_{\mathcal{B}_k \subseteq \mathbf{B}} \psi(\mathcal{B}_k) \quad (2)$$

$$\psi(\mathcal{B}_k) = \frac{\min\{\text{vol}(\mathcal{B}_k), \text{vol}(\bar{\mathcal{B}}_k)\}}{\text{div}(\mathcal{B}_k, \bar{\mathcal{B}}_k)} \quad (3)$$

$$\text{div}(\mathcal{B}_k, \bar{\mathcal{B}}_k) = \frac{|\sum \vec{e}_j|}{|\mathcal{E}(\mathcal{B}_k, \bar{\mathcal{B}}_k)|}, e_j \in \mathcal{E}(\mathcal{B}_k, \bar{\mathcal{B}}_k) \quad (4)$$

Subject to

$$|\mathcal{B}_k| < \frac{1 + \epsilon}{N_B} \bigcup_{k=1}^{N_B} |\mathcal{B}_k| \quad (5)$$

$$D_{min} \leq D(\mathcal{B}_k) \leq D_{max} \quad (6)$$

where $\psi(\mathcal{B}_k)$ is our proposed **Connection Quality Score (CQS)** for block \mathcal{B}_k , a metric designed to capture the core principles of high cohesion, low coupling, and dispersed directional connectivity during the block evolution. Here, $\text{vol}(\mathcal{B}_k)$ denotes the volume of block \mathcal{B}_k , defined as the sum of the degrees of all nodes within \mathcal{B}_k , and $\text{div}(\cdot)$ is the directional connectivity. \vec{e}_j is the unit vector representing the direction of an IUL, and $\mathcal{E}(\mathcal{B}_k, \bar{\mathcal{B}}_k)$ is the set of IULs of block \mathcal{B}_k . Constraint (5) ensures balanced block sizes, and (6) bounds the block diameter, where ϵ is the error constant.

The CQS metric $\psi(\mathcal{B}_k)$ is designed to meet our survivability objectives by promoting high internal connectivity (through $\min(\text{vol})$) to enhance block stability when encountering internal failures, preventing frequent shrink or expansion, and by encouraging evenly distributed external links across directions (through low div) to provide more diversified forwarding options, thereby improving path diversity during routing selection. This focus on directional diversity is more critical for survivability than merely having a high number of links, as it prevents over-reliance on a single direction.

The SLP problem is NP-hard as it generalizes the Max-Cut problem [5]. Given the volatility of LSNs, centralized partitioning is impractical. Therefore, we employ a distributed heuristic algorithm (Algorithm.1) to find feasible solutions in polynomial time.

4.3 SLP Problem Solving

To address the SLP problem, we propose a distributed **CQS**-aware **Block Evolution** (**CQSBE**) algorithm, which operates within the control plane of each block under the maintenance framework of DABNet. As illustrated in Algorithm.1, the CQSBE dynamically adapts to both intra-block and inter-block network conditions while maintaining an optimal block size.

Algorithm 1: Distributed CQS-aware Block Evolution Algorithm (CQSBE)

Input: Block \mathcal{B}_k
Output: Evolved block \mathcal{B}_k^*

```

1 if Diameter( $\mathcal{B}_k$ )  $<$   $D_{max}$  then
2    $\mathcal{S}_{adj} \leftarrow \text{Adj}(\mathcal{B}_k)$ ;  $\mathbf{B} \leftarrow \emptyset$ ; // block expansion
3   for  $s_j \in \mathcal{S}_{adj}$  && State( $s_j$ ) = VAGRANT do
4      $\mathcal{B}' \leftarrow \mathcal{B}_k + s_j + \mathcal{E}(s_j, \mathcal{B}')$ ;  $\mathbf{B} \leftarrow \mathbf{B} \cup \mathcal{B}'$ ;
5   end
6    $\mathcal{B}_k^* \leftarrow \underset{\mathcal{B}' \in \mathbf{B}}{\text{argmax}} \psi(\mathcal{B}')$ ;
7 else
8   // block shrink
9    $s_r \leftarrow \underset{s \in \mathcal{S}^*}{\text{argmin}} \phi(s, \mathcal{B}_k)$ ;  $\mathcal{B}_k^* \leftarrow \mathcal{B}_k - s_r$ ;
9 end
10 return  $\mathcal{B}_k^*$ 
```

During the evolution process, the block evaluates potential connectivity improvements by tentatively computing betweenness-centrality ψ through simulated merges with neighboring VAGRANT satellites. The candidate blocks \mathcal{B}' exhibiting maximal ψ values are selected as optimal evolution targets \mathcal{B}^* (lines 6-11). Concurrently, when the block diameter exceeds the predefined threshold D_{max} due to failure or congestion, the block adaptively runs shrink operation by removing the satellite with the lowest closeness-centrality ϕ , thereby ensuring the block maintains an appropriate scale. The closeness-centrality ϕ is formulated as

$$\phi(u, \mathcal{B}) = \frac{N_{\mathcal{B}} - 1}{\sum_{u \neq v, u, v \in \mathcal{B}} d(u, v)} \quad (7)$$

where $d(u, v)$ denotes the hop-count of the shortest path between vertices u and v , and $N_{\mathcal{B}}$ represents the number of vertices in block \mathcal{B} .

For performance evaluation, we implement a **RANDOM** baseline strategy that differs from CQSBE solely in its stochastic selection of inner-block satellite removals and VAGRANT satel-

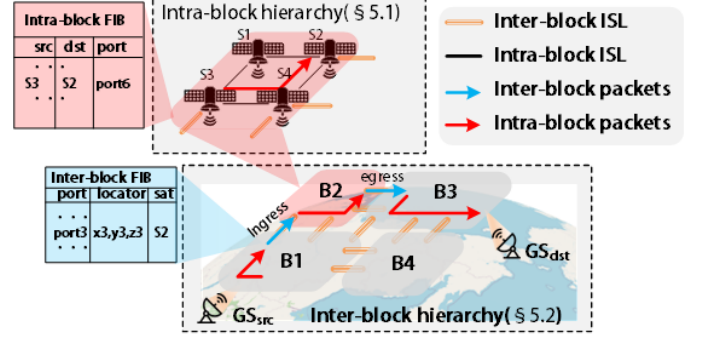


Figure 5: The hierarchical routing architecture in BlockFlex.

lite merges during shrinkage/expansion, rather than employing the ψ and ϕ criterions for guided decision-making.

5 Hierarchical Routing over DABNet

BlockFlex integrates a hierarchical routing scheme (DABR) over DABNet, and Fig.5 presents an overview of DABR's architecture. The entire DABR consists of inter-block routing (§5.1) and intra-block routing (§5.2), which enables packet forwarding based on inter-block FIBs and intra-block FIBs maintained by each block respectively. We assume that each block has a separate control plane and operates on any satellite within the block. Under DABNet's stable network abstraction, DABR employs convergence-free geographic routing hierarchy by utilizing pose information maintained within forwarding units (§5.1) and a convergence-isolated centralized routing hierarchy integrated with individual block's evolution (§5.2). Additionally, to address the dead-end issue inherent in geographic routing [20, 59] and the instability caused by multipath routing, DABR incorporates a synchronized forwarding cache mechanism (§5.3) and a source satellite stability selection algorithm (§5.4) to mitigate them respectively. We next describe the components in detail.

5.1 Inter-blocks Routing

Geographic routing between forwarding units.

To ensure routing efficiency through global convergence-free operation, we develop a geographic routing scheme for packet forwarding between blocks and vagrant satellites. Each forwarding unit utilizes the Global Navigation Satellite System (GNSS) [22, 63] to obtain real-time location and orientation information for itself and its neighbors. Based on this information, three forwarding criteria are implemented to determine the egress port link e_{egress} (i.e., the next-hop forwarding unit):

Closer to Target Vertex (CTV):

$$e_{egress} = \underset{e_i \in E}{\text{argmin}} \{ |\vec{e}_i + \vec{r}(s_j) - \vec{r}_{dst}| \} \quad (8)$$

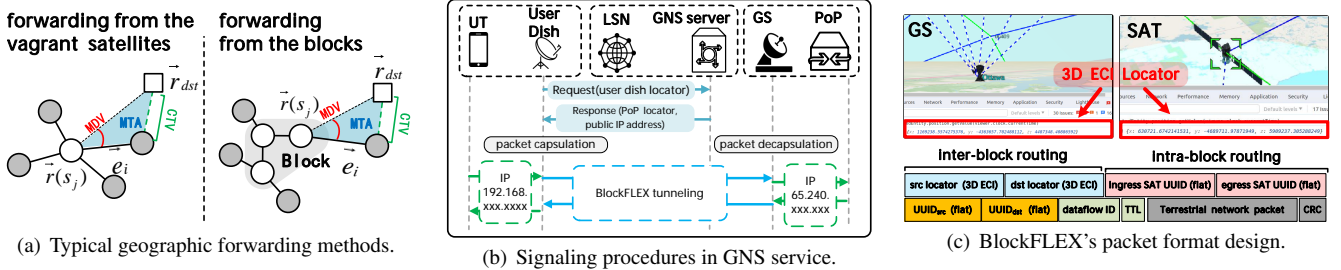


Figure 6: Components of geographic routing in blockFLEX.

Minimum Deviation Vertex (MDV):

$$e_{\text{egress}} = \underset{e_i \in \mathcal{E}}{\operatorname{argmin}} \left\{ \frac{\vec{e}_i \cdot (\vec{r}_{\text{dst}} - \vec{r}(s_j))}{|\vec{e}_i| |\vec{r}_{\text{dst}} - \vec{r}(s_j)|} \right\} \quad (9)$$

Minimum Triangle Area (MTA):

$$e_{\text{egress}} = \underset{e_i \in \mathcal{E}}{\operatorname{argmax}} \left\{ \frac{\vec{e}_i \cdot (\vec{r}_{\text{dst}} - \vec{r}(s_j))}{|\vec{e}_i| |\vec{r}_{\text{dst}} - \vec{r}(s_j)| |\vec{e}_i + \vec{r}(s_j) - \vec{r}_{\text{dst}}|} \right\} \quad (10)$$

Here, \mathcal{E} denotes the set of all possible egress ISLs in the current forwarding unit; s_j and $r(s_j)$ represent the locator and position vector of the current forwarding unit, respectively; and r_{dst} is the position vector of the destination ground station g_{dst} . In summary, most geographic routing schemes [20, 28, 33, 35, 41, 55, 62] determine the next hop based on the triangular geometric relationship among the current node’s location, the candidate next-hop node’s location, and the destination node’s location, as illustrated in Fig. 6 (a), where \bullet and \blacksquare denote satellites and ground stations, respectively.

Locator-Identifier Decoupling. Traditional terrestrial networks (e.g., IP-based architectures) tightly couple network locators and identifiers, complicating mobility management and limiting scalability. In LSNs, the edge nodes exhibit vastly different mobility patterns, ranging from stationary GSes to high-speed remote sensing satellites. Furthermore, the network itself gradually expands with ongoing deployment, necessitating inherent scalability. Therefore, BlockFLEX decouples network addresses into locators and identifiers [11]. As shown in Fig. 6(b), before establishing an end-to-end session, the sender (user dish) sends a request to the locally recorded Global Name Service (GNS) server a known locator to resolve the destination’s static flat network identifier into an addressable locator. The GNS serves as a critical name-resolution infrastructure for network addressing. Upon receiving the request from the sender, the GNS returns the locator of the destination node (GS) and leases a public IP address to the source node. After obtaining this information, the sender utilizes its local NAT server to translate its private IP address into the assigned public address. It then encapsulates both the public source IP address and the destination locator into a BlockFLEX datagram and starts the communication session.

This service architecture works similarly to DNS services [40] and is generally deployed in a distributed manner around the globe; the feasibility of such an approach has been explored in the MobilityFirst architecture [57]. Some high-speed moving objects, on the other hand, periodically send location information back to the GNS server during the networking process to maintain their network addressability. In this way, the flat identifier and structured locator can satisfy the scalability requirements of emerging LSNs while accomplishing efficient addressing. This architecture enables BlockFLEX to function as a tunnelling sub-layer [45], facilitating interoperability across diverse terrestrial network protocols.

Transparent Addressing via Earth-Centered Inertial Coordinate System. As part of the locator design introduced earlier, we further propose a transparent addressing mechanism to enhance flexibility and scalability under dynamic network conditions. Existing works [8, 26, 28, 29, 33, 35, 37, 64] handle the Earth-satellite dynamics in LSNs through complex addressing schemes such as incorporating satellite orbital/shell information or ground-partition-guided satellite addressing. However, the inflexible address space brings great challenges to the scalability of the network. To overcome this, we introduce the concept of **transparent addressing**, in which the network locator remains invariant throughout packet forwarding, rendering the addressing process effectively invisible to BlockFLEX without requiring awareness of Earth-satellite relative motion. We observe that recent complex addressing mechanisms [29, 33] aim to **establish a nonlinear mapping between terrestrial and space locators** under highly dynamic conditions. This can be achieved through the Earth-Centered Inertial (ECI) coordinate system [49], which provides a three-dimensional inertial reference frame fixed in space, independent of Earth’s rotation. By utilizing on-board GNSS receivers, satellites can perform addressing in the Earth-Centered Inertial (ECI) coordinate system using static locators (such as latitude and longitude). This method not only eliminates distortions caused by Earth’s rotation but also capitalizes on the continuous nature of the coordinate space to achieve excellent scalability.

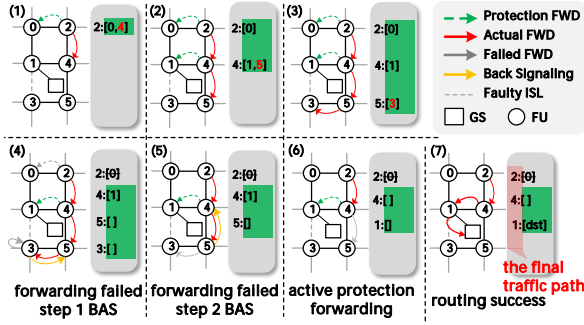


Figure 7: The n-steps backward acknowledgment signalling.

5.2 Intra-block Routing

The concept of network partitioning into isolated convergence domains has been extensively studied in the literature [3, 30, 46]. This approach not only enhances convergence speed and reduces overhead but also mitigates global routing oscillations while significantly improving network scalability. The inherent topological characteristics of LSN determine their flat architecture [33]. However, the number of nodes in LSN is expected to grow exponentially in the foreseeable future. Therefore, introducing a convergence-isolated mechanism not only improves routing efficiency but also holds critical importance for network scalability. Unlike some multi-layer satellite network hierarchical routing [10, 33, 39], the abstraction in DABNet does not need to consider the number of shells of the actual satellite network. The routing re-convergence within a block is triggered when the block re-evolves due to failures or internal traffic congestion. Block will dynamically update intra-block FIB according to the internal traffic situation, and topology changes, and utilize the Link State Advertisement [12] mechanism for the optimal path between any satellites within the block. Since blocks are constrained to a small size, control messages remain confined within the block even under frequent failures or traffic fluctuations, preventing excessive overhead.

5.3 Protection Routing Mechanism.

Geographic routing offers high efficiency due to its convergence-free nature. However, it cannot guarantee route reachability and may suffer from last-hop ambiguity or local minima [20, 35, 55, 60], where addressing fails near the destination, leading to packet loss. To address this, we propose a protection routing method based on the **n**-steps **B**ackward **A**cknowledgment **S**ignaling (**nBAS**) mechanism. Each forwarding unit (FU) along the path of dataflow I_D maintains a protection forwarding stack (PFS) $\mathcal{P}[I_D]$, which stores all feasible next-hop options. If routing fails, a backward signaling process is triggered recursively to retrieve cached alternatives and activate backup paths. The nBAS mechanism operates in

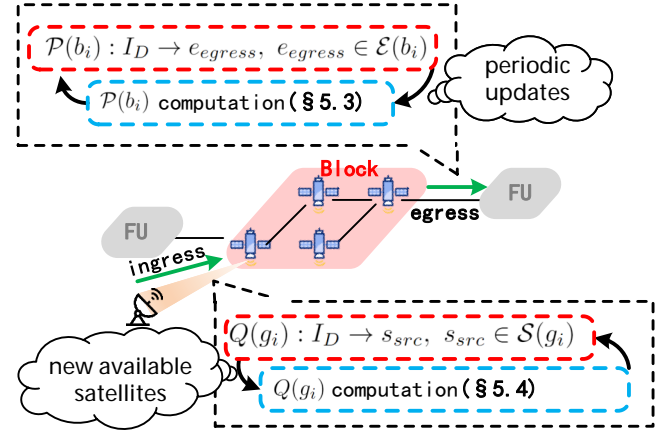


Figure 8: Dual-mode forwarding policy.

three steps: (see Fig. 7):

❶ PFS initialization/update: As the dataflow travels (e.g., $U_2 \rightarrow U_4 \rightarrow U_5$), each FU computes and ranks all possible egress links by a geographic matching score (Eq. 8–10), storing them in the PFS, not just the optimal next hop.

❷ Failure handling: When a FU U_3 fails to forward packet in I_D , it checks its PFS. If empty, a NACK is sent upstream to U_5 . If that PFS is also empty, the signal continues to U_4 (two-hop fallback).

❸ Protection forwarding active: Once a unit with a non-empty PFS (e.g., U_4) is reached, it pops a backup forwarding (e.g., $U_4 \rightarrow U_1$), confirms adjacency to the destination ground station g_{dst} , and redirects traffic via $U_1 \rightarrow g_{dst}$.

The nBAS mechanism operates in a distributed manner, with each Forwarding Unit (FU) independently making decisions based on its local Protection Forwarding Stack (PFS) and recursively propagating NACK signals. By leveraging limited-step backtracking without global topology information, nBAS effectively implements a form of distributed depth-first search to achieve efficient path recovery.

5.4 Optimal Source Satellites Selection

The GS in LSN maintains continuous coverage from multiple satellites and appropriate source/destination satellite selection during routing can yield significant performance improvements [17, 36, 64]. However, identifying the optimal path between source/destination satellites sets typically requires centralized control-plane intelligence and cannot be feasibly accomplished in a purely distributed manner. To overcome this limitation while mitigating the instability introduced by BlockFLEX's use of a larger satellite set for establishing traffic paths, we focus specifically on source satellite selection and propose the **Optimal Source Satellite Selection** algorithm (**OS3**). Specifically, each GS maintains a Source-satellite Priority Queue (SPQ) $Q[I_D]$ for each dataflow I_D to store the optimal source satellites for I_D , which are prioritized accord-

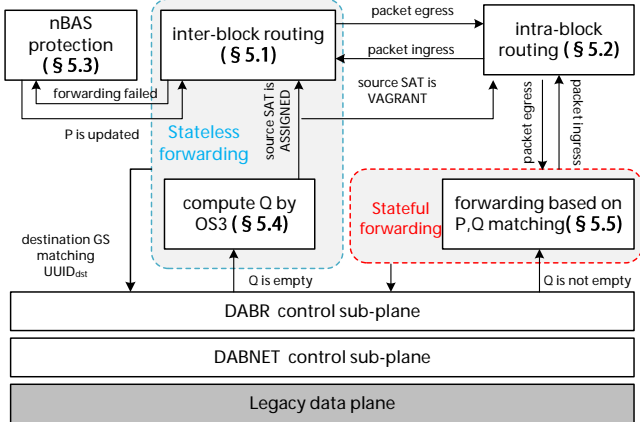


Figure 9: The BlockFLEX overlay.

ing to the latest RTT of the I_D . The RTTs are collected by randomly selecting source satellites during the initial phase of the dataflow, and $Q[I_D]$ will be dynamically updated as available satellites change. As the dataflow continues, it will gradually converge toward the source satellite with the optimal RTT. More details of OS3 are shown in § Appendix.B.

5.5 System Integration

Inter-block routing based on geographic policy (§ 5.1) represents a typical stateless forwarding mechanism, where each forwarding decision is made independently of connection state and relies solely on the header information of the current packet. In contrast, the protection routing mechanism (§ 5.3) and the source satellite selection policy (§ 5.4) require maintaining connection-specific information (such as dataflow identifier I_D) and leveraging cached context (P and Q), constituting a stateful forwarding approach. To reconcile this difference, we introduce a dual-mode switching architecture that dynamically switches between stateful and stateless operations. As illustrated in Fig. 8, this architecture separates the forwarding process into computation phase and a matching phase.

During the computation phase, forwarding units operate in stateless mode (blue boxes). In this mode, the detection of newly available source satellites s_{src} triggers the computation of the source-satellite priority queue Q , while periodic updates of the protection forwarding stack P are performed based on current network conditions. In the matching phase, all nodes switch to stateful mode (red boxes). Here, ground stations (GS) and forwarding units utilize the precomputed P and Q to perform efficient lookup-based forwarding. This hybrid approach reduces computational overhead during packet processing [54], while retaining the performance benefits of convergence-free geographic routing. By integrating the mechanisms described in § 5.1–§ 5.5, we establish the complete control plane of BlockFlex, as depicted in Fig. 9.

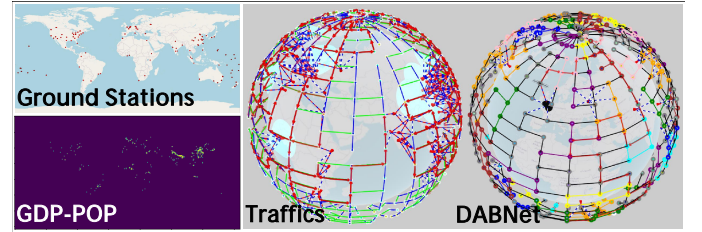


Figure 10: The implementation and experimental workloads.

6 Implementation

We implement the BlockFlex’s prototype using an open-source time-driven simulator SNK [61], which provides comprehensive support for large-scale constellation network simulation and routing scheme test, as is shown in Fig. 10. The implementation extends the `snklib.network_scheme` class with 500 lines of Python code to realize DABNet, where each forwarding unit operates in an independent thread to perform block evolution and internal routing convergence. When satellites merge into a block, one of them is randomly selected as the controller while terminating threads of the remaining satellites. Similarly, we implement DABR with 600 lines of Python code under the `snklib.route_scheme` class. For system observability, we develop real-time evolutionary process visualization through the `snklib.animation` module, encoding satellite state transitions and traffic dataflows into an `animation_list` for rendering in SNK’s frontend monitoring subsystem (`snk-visualizer`), enabling dynamic debugging of BlockFlex’s adaptation and routing behaviors. Our evaluation employs analysis scripts leveraging SNK’s built-in functions to process generated instance data and draw the chart. All the simulations executed on a hardware platform featuring an Intel Core i7-10700K processor, 32GB RAM, and NVIDIA GeForce GTX 2080 Ti GPU.

7 Evaluation

We evaluate the performance of our BlockFlex implementation and compare it against several existing LSN routing schemes across four key aspects: survivability (§ 7.1), resiliency (§ 7.2), efficiency (§ 7.3), and latency/stability (§ 7.4). The experimental setup is described as follows:

► **Constellations:** Our experiments are based on two operational satellite Internet constellations: Starlink [50] and OneWeb [13]. We simulate the complete first shell of Starlink, consisting of 1584 satellites distributed across 72 orbital planes at an altitude of 550 km. Similarly, we simulate the OneWeb constellation as approved by the FCC [13], which comprises 588 satellites in 12 orbital planes. All scenarios employ the +Grid ISL structure [4].

► **Network failure model:** We model ISL failures under multiple LSN scenarios with failure ratios ranging from 0% to 30%. All failures are modeled as unpredictable events,

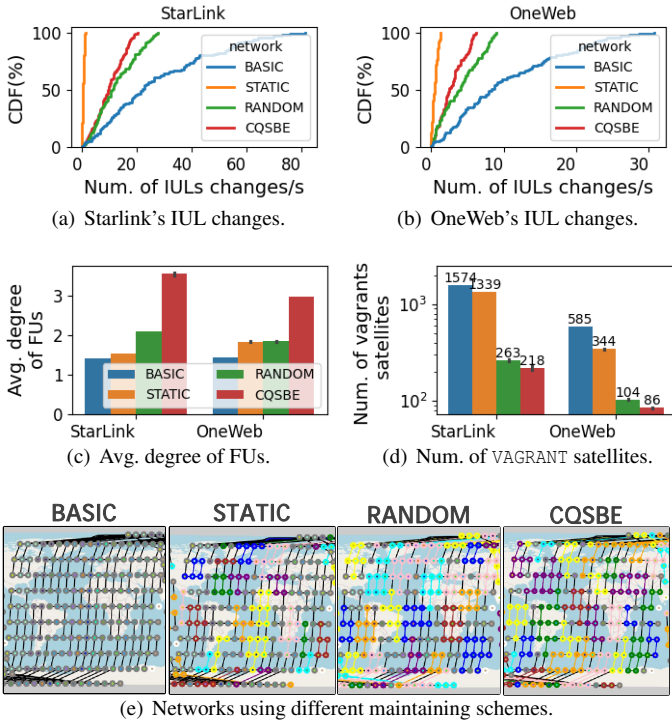


Figure 11: Network survivability under 30% ISL failures using different network maintaining schemes.

with each ISL connection and disconnection occurring randomly and following a uniform distribution in duration to simulate stochastic link availability. More details are shown in § Appendix.D.

► **Traffic scheme:** We select over 100 major cities and islands as ground station (GS) locations. Traffic demands are generated based on a weighted average of Gross Domestic Product (GDP) and population, where the weight determines the probability of traffic generation between pairs. Over a period of 2000 seconds, we generate more than 1000 source-destination GS pairs as traffic flows, as illustrated in Fig. 10.

► **Routing schemes:** We re-implemented SHORT [33] and OrbitCast [29] based on the descriptions in their original papers. For OSPF [12] and ADOV [44] protocols, we compute routes using Dijkstra’s algorithm via the networkx package [19], and derive corresponding costs by incorporating their routing characteristics with the dynamic network topology.

7.1 Survivability in DABNet’s Topology View

As the underlay of routing, DABNet’s survivability refers to its capability to maintain a stable topological view despite the volatility of LSNs (Low Earth Orbit Satellite Networks), thereby providing a foundation for reliable routing in the overlay network. Accordingly, our evaluation quantifies three key metrics under 30% ISL failures: the number of

IUL changes, the count of vagrant satellites, and the average node degree, which collectively demonstrate DABNet’s survivability performance. The comparing schemes include: 1) **BASIC**: Conventional satellite networks, 2) **STATIC**: DABNet without evolutionary adaptation after initialization, 3) **RANDOM**: DABNet employing random evolution strategies, and 4) **CQSBE**: DABNet evolved using the CQSBE algorithm (§4.3).

By imposing more coordinated constraints on block expansion and shrink, CQSBE maintains lower connectivity variations between forwarding units compared to random evolution, thereby enabling DABNet to evolve with higher stability, as is shown in Fig. 11 (a). For conventional satellite network architectures, any link failure leads to topological changes, resulting in maximal topological dynamics. For static DABNet (where evolution is paused), only network failures can trigger topological changes, thus maintaining minimal dynamics. In Fig. 11 (b), we observe that compared to the RANDOM evolution, the CQSBE method results in blocks with higher average degrees in DABNet and better utilizes vagrant satellites for merging. Fig. 12 (c) illustrate different network schemes in the OneWeb constellation. We observe that CQSBE generates more blocks (colored nodes) while maintaining fewer vagrant satellites (gray node). Evidently, under severe faulty networks, DABNet with CQSBE method exhibits more stable evolution and improved satellite partitioning by remaining less vagrant satellites. This further mitigate the impact to overlay network, thereby providing the basis of survivable architecture.

7.2 Routing Resiliency

Table 2 summarizes the reachability performance of various routing schemes under different ISL failure ratios for both Starlink and OneWeb constellations. The experimental results are systematically categorized into four groups to facilitate comparative analysis. The first group comprises two state-of-the-art LSN routing schemes, OrbitCast [29] and SHORT [33], which serve as baseline comparisons. Both schemes exhibit significant performance degradation with increasing failure ratios, reaching approximately 44-49% reachability under 30% failure conditions. The second group evaluates the BlockFLEX framework employing three distinct geographic forwarding policies (MDV, CTV, MTA) as inter-block routing algorithms (see §5.1), with DABNet undergoing random evolution. These implementations demonstrate notably improved resilience, achieving 51-61% reachability at 30% failure ratio, representing a substantial improvement over baseline schemes. The third group incorporates the CQSBE algorithm into DABNet evolution in the BlockFLEX framework, resulting in further performance enhancements. The integration of CQSBE yields reachability values of 63-64% for Starlink and 55-63% for OneWeb under 30% failure conditions, confirming the effectiveness of strategic block evolution in improving network survivability. The fourth group presents the complete pro-

Table 2: Reachability of different routing schemes.

Routing schemes	Failure ratio				Starlink				OneWeb			
	0%	10%	20%	30%	0%	10%	20%	30%	0%	10%	20%	30%
OrbitCast [29]	94.54 (± 1.10)	77.27 (± 2.01)	62.62 (± 2.63)	46.13 (± 3.07)	97.21 (± 0.48)	81.45 (± 3.15)	64.94 (± 2.77)	45.70 (± 1.54)	97.55 (± 0.89)	79.09 (± 2.62)	65.55 (± 5.19)	49.01 (± 2.68)
SHORT [33]	97.55 (± 0.89)	79.09 (± 2.62)	65.55 (± 5.19)	49.01 (± 2.68)	97.70 (± 0.72)	82.29 (± 2.44)	64.62 (± 3.49)	44.98 (± 1.85)	97.55 (± 0.89)	79.09 (± 2.62)	65.55 (± 5.19)	49.01 (± 2.68)
DABR(MDV)	93.85 (± 1.01)	84.15 (± 1.77)	73.64 (± 2.44)	60.10 (± 2.24)	90.83 (± 1.43)	79.77 (± 1.99)	71.08 (± 2.71)	51.64 (± 3.53)	94.14 (± 0.67)	82.66 (± 1.78)	75.06 (± 1.67)	59.40 (± 1.93)
DABR(CTV)	94.14 (± 0.67)	82.66 (± 1.78)	75.06 (± 1.67)	59.40 (± 1.93)	91.67 (± 1.05)	81.34 (± 2.80)	73.69 (± 2.39)	56.38 (± 2.24)	93.64 (± 0.93)	83.92 (± 1.58)	73.42 (± 2.28)	61.29 (± 2.09)
DABR(MTA)	93.64 (± 0.93)	83.92 (± 1.58)	73.42 (± 2.28)	61.29 (± 2.09)	90.82 (± 1.37)	80.95 (± 2.59)	71.77 (± 2.80)	53.29 (± 3.33)	96.18 (± 1.21)	88.58 (± 2.64)	79.08 (± 4.87)	63.03 (± 2.05)
DABR(MDV)+CQSBE	96.18 (± 1.21)	88.58 (± 2.64)	79.08 (± 4.87)	63.03 (± 2.05)	91.89 (± 1.43)	84.87 (± 4.42)	70.76 (± 2.38)	55.22 (± 3.30)	96.75 (± 0.61)	89.81 (± 2.81)	81.56 (± 4.41)	64.56 (± 4.78)
DABR(CTV)+CQSBE	96.75 (± 0.61)	89.81 (± 2.81)	81.56 (± 4.41)	64.56 (± 4.78)	96.15 (± 0.68)	84.60 (± 2.75)	73.85 (± 2.09)	63.76 (± 2.55)	97.16 (± 0.81)	88.74 (± 2.04)	83.10 (± 3.07)	64.37 (± 4.67)
DABR(MTA)+CQSBE	97.16 (± 0.81)	88.74 (± 2.04)	83.10 (± 3.07)	64.37 (± 4.67)	94.81 (± 0.98)	84.47 (± 3.46)	72.74 (± 1.89)	63.18 (± 2.51)	100 (± 0.00)	99.98 (± 0.04)	99.95 (± 0.01)	98.37 (± 0.08)
DABR(MDV)+CQSBE+nBAS	100 (± 0.00)	99.98 (± 0.04)	99.95 (± 0.01)	98.37 (± 0.08)	99.80 (± 0.20)	99.72 (± 0.26)	98.36 (± 0.54)	93.72 (± 1.60)	100 (± 0.00)	100 (± 0.00)	99.94 (± 0.01)	98.72 (± 0.10)
DABR(CTV)+CQSBE+nBAS	100 (± 0.00)	100 (± 0.00)	99.94 (± 0.01)	98.72 (± 0.10)	99.90 (± 0.15)	99.76 (± 0.20)	98.68 (± 0.40)	95.25 (± 1.37)	100 (± 0.00)	100 (± 0.00)	99.96 (± 0.01)	98.68 (± 0.09)
DABR(MTA)+CQSBE+nBAS	100 (± 0.00)	100 (± 0.00)	99.96 (± 0.01)	98.68 (± 0.09)	99.89 (± 0.13)	99.73 (± 0.24)	98.50 (± 0.40)	93.18 (± 1.29)				

Bold numbers indicate optimal results, while underlined numbers denote sub-optimal results.

posed solution, integrating the nBAS route protection mechanism with the CQSBE-enhanced BlockFLEX framework. This comprehensive approach demonstrates remarkable resiliency, maintaining near-perfect reachability (99.9-100%) under minor failures and achieving outstanding performance of 93-98% even under severe (30%) failure conditions. Notably, DABR(CTV)+CQSBE+nBAS achieves optimal performance across most scenarios, reaching 95.25% and 98.72% reachability for OneWeb and Starlink respectively at 30% failure ratio.

The comparative analysis reveals a progressive performance improvement through the sequential integration of proposed techniques. The complete solution shows a 35.7% average reachability improvement over baseline schemes and a 2 \times enhancement under severe ISL failure conditions, conclusively demonstrating the effectiveness of the BlockFLEX architecture in maintaining communication resiliency in volatile LSN environments.

7.3 Routing Efficiency

Routing rediscovery. Fig.12(a) compares the number of routing rediscovery events of each dataflow among state of the art geographic routing schemes, namely OrbitCast [29] and SHORT [33], against BlockFLEX and their nBAS augmented variants. While the nBAS protection mechanism substantially improves routing reachability, it also introduces additional rediscovery procedures. The baseline OrbitCast, SHORT and BlockFLEX schemes exhibit no rediscovery, maintaining a count of zero. In contrast, enabling nBAS triggers protection routing through the cached PFS upon packet delivery failure, which activates rediscovery operations. In our experiments, the maximum number of backward acknowledgment attempts per route was uniformly set as $n_{\max} = 5$. Compared to the nBAS enhanced versions of OrbitCast and SHORT, BlockFLEX's aggregation of forwarding satellites into blocks

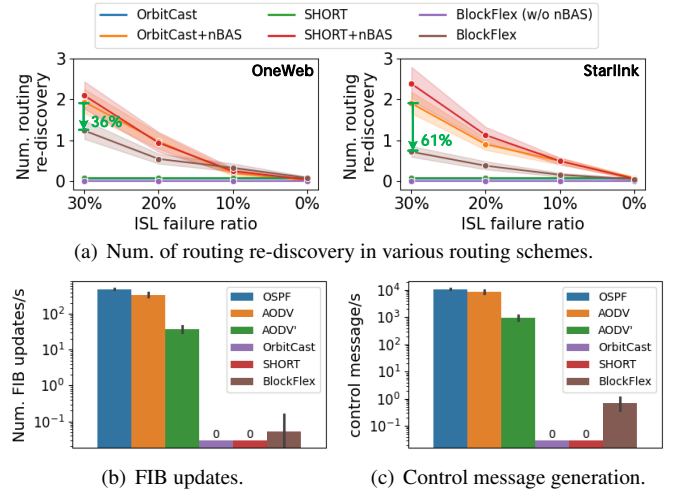
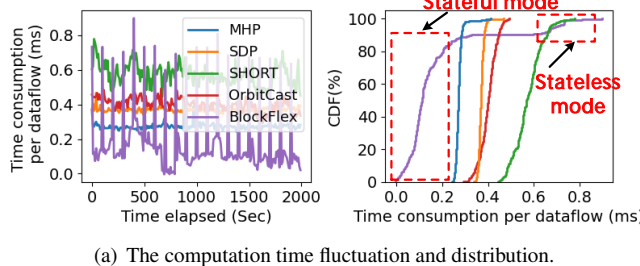


Figure 12: Routing overheads.

reduces the number of fallback signaling processes during protection forwarding. Compared to the suboptimal method (OrbitCast), the proposed BlockFLEX scheme achieves a reduction in average routing rediscovery count of 36% (1.23 vs. 1.93) on OneWeb and 61% (0.32 vs. 0.84) on Starlink, thereby lowering overall routing overhead.

Routing Convergence. In Fig.12 (b) and (c), we quantify routing convergence overhead by counting topology changes and the number of nodes within the convergence scope, while considering protocol-specific characteristics to compute the frequency of Forwarding Information Base (FIB) updates and the number of control messages generated during convergence. All routing schemes in the simulation experience the same traffic load, except AODV', which operates at 50% of the load of other schemes. Due to satellite-to-ground station dynamics and intermittent ISL failures, OSPF triggers frequent network-wide FIB updates and floods the system with excess



(a) The computation time fluctuation and distribution.

	MHP	SDP	SHORT	OrbitCast	BlockFLEX
Time (ms)	0.272	0.369	0.572	0.399	0.174
Std (ms)	±0.017	±0.012	±0.036	±0.061	±0.189

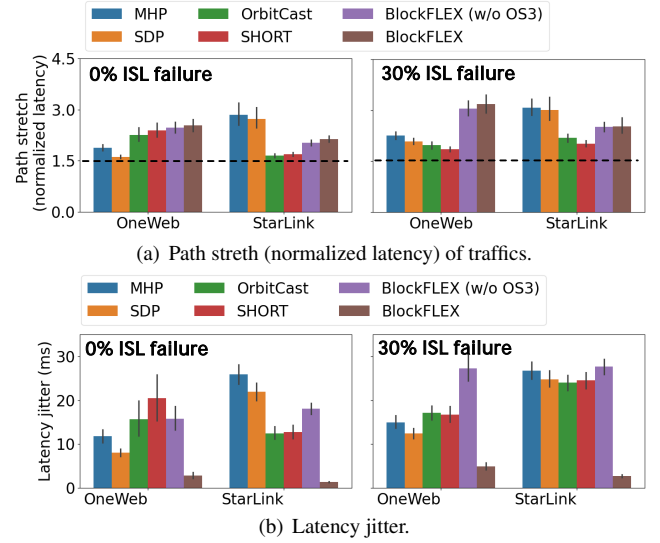
(b) Avg. time consumption per dataflow.

Figure 13: Routing Computation Time.

sive control messages. AODV, with its on-demand routing nature, incurs significantly lower overhead than OSPF at 50% load—approximately 10% of OSPF’s overhead (green bar). However, its overhead approaches that of OSPF as traffic load increases to the same level. OrbitCast [29] and SHORT [33] leverage stateless forwarding and convergence-free routing, resulting in zero FIB updates and control message generation. Instead, BlockFLEX confines convergence to localized blocks, maintaining 0.2% FIB update frequency and 0.1% control message overhead relative to OSPF. While convergence-free schemes achieve zero overhead, BlockFLEX significantly outperforms convergent protocols like OSPF and AODV, despite geographic routing’s resilience limitations as shown in §7.2.

Routing computation time consumption. This section analyzes the time consumption of routing computation under a fixed dataflow configuration, with the PFS update interval in BlockFLEX set to $\delta = 100$ s. We measure only the computational overhead during the path selection phase. Both the Minimum Hop-count Path (MHP) and Shortest Distance Path (SDP) are computed using the networkx library [19]. These two path selection methods are widely adopted in protocols such as AODV [44] and OSPF [12]. As illustrated in Fig.13, despite operating on networks with thousands of nodes, both MHP and SDP maintain exceptionally low computational overhead via the networkx library. Within geographic routing schemes, SHORT requires more time than OrbitCast due to its denser vector operations.

In BlockFLEX, Fig.13 (left) reveals a periodic pattern in computation time, with cycles corresponding to the predefined PFS recomputation interval ($\delta = 100$ s). Fig.13 (right) demonstrates that the stateful mode maintains low computation time, as next-hop decisions are efficiently determined through simple table lookups. In contrast, the stateless mode incurs substantially higher computational overhead, as each satellite along the traffic path must perform computationally intensive geographic-based PFS calculations. In our experiments, the SPQ Q computation is triggered by newly adjacent



(a) Path stretch (normalized latency) of traffics.

(b) Latency jitter.

Figure 14: Latency and path stability.

source satellite sets. Its time cost is negligible compared to PFS recomputation, resulting in less noticeable periodicity. As clearly demonstrated in Fig.13 (b), BlockFLEX exhibits significant computational efficiency: it achieves average computation time reductions of 56% and 36% compared to geographic routing (OrbitCast) and shortest-path routing (MHP), respectively. Additionally, it is anticipated that as update interval in BlockFLEX δ increases, the overall computational overhead will decrease due to reduced spatial computations; however, this will result in degraded routing reachability.

7.4 Latency and stability

Macroscopic performance analysis. Fig.14 compares the one-way propagation latency across different routing schemes. Path stretch, defined as the ratio between the actual path length and the geographic distance, serves as a normalized latency metric [4, 23]. Since the speed of light in optical fiber is approximately $2c/3$, where c represents the speed of light in vacuum, any stretch value below 1.5 (as indicated by the dashed line in Fig. 14(a)) implies performance exceeding that of terrestrial direct fiber links.

Compared to shortest-path routing (SDP, MHP) and geographic routing (SHORT, OrbitCast), BlockFLEX does not exhibit significant advantages in latency, yet it achieves comparable results. This can be attributed to two main factors. First, BlockFLEX considers a larger set of satellites during path selection, enhancing path diversity but also increasing the likelihood of higher-latency paths. Second, conventional average latency metrics often exclude routing failures, which occur frequently in low satellite networks (LSN) as discussed in §7.2, potentially leading to underestimated latency values. Additionally, we note that after incorporating the OS3 mechanism, BlockFLEX does not exhibit a significant advantage in

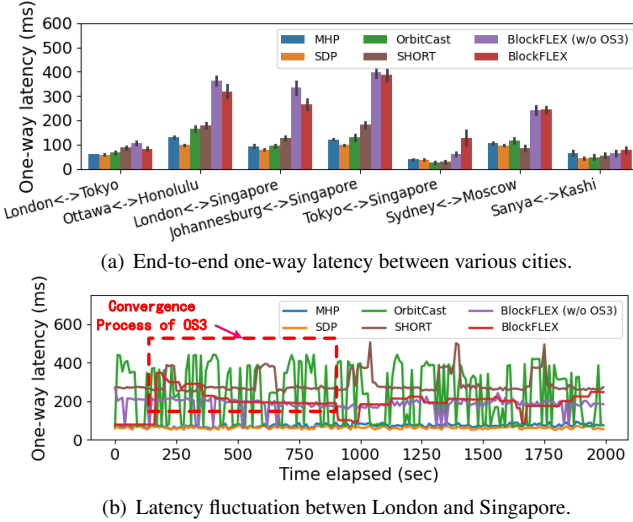


Figure 15: Latency in end-to-end session.

latency. We attribute this to the fact that while OS3 stabilizes path diversity, it also excludes certain source satellites that, despite having shorter available time windows, could provide shorter paths.

Nevertheless, BlockFLEX demonstrates superior performance in terms of latency jitter in Fig. 14 (b). It reduces jitter by at least 50% compared to the second-best scheme, with further improvements observed under higher ISL failure. For example, in the Starlink scenario with 30% ISL failure, BlockFLEX achieves an 88% reduction in latency jitter relative to conventional routing schemes.

Microscopic performance analysis. The Fig. 15 (a) presents several selected dataflow results from the OneWeb constellation, while Fig. 15 (b) shows the latency fluctuation between London and Singapore. As can be observed, the geographic routing scheme may fall into local optima during the addressing process, leading to significant instability. Particularly under the OrbitCast method, this can introduce jitter exceeding 300ms. Our proposed BlockFLEX algorithm scheme optimal source satellite ranking and selection during its initial operation phase, then gradually converges to the optimal choice with the lowest relative latency, as demonstrated in the right panel of Fig. 15 (b). Consequently, LSN employing the BlockFLEX can effectively mitigate packet reordering phenomena, thereby significantly enhancing Quality of Service (QoS) for delay-sensitive applications such as streaming media services.

8 Related works

LSN Routing. The simplest LSN routing approach mirrors terrestrial methods, using centralized computation to achieve

global FIB convergence¹. Alternatively, the prediction-based methods [18, 28, 43] can reduce convergence overhead but still struggle to support large-scale user routing. Recent studies [28, 29, 33, 35, 64] rethink LSN architecture holistically, employing stateless, convergence-free geographic routing to improve resiliency, stability, and scalability while reducing control overhead.

Masking the volatility in LSNs. To mitigate network volatility, virtualization-based approaches [8, 26, 37] abstract physical infrastructures into virtual topologies or nodes, replacing global routing convergence with localized container switching. While this reduces the problem to a near-static topology level, the significant latency and bandwidth overhead of container switching continue to challenge service availability in LSNs. Complementing these efforts, recent topology-stabilizing models [28] conceptualize link failures as an extreme form of congestion. By providing routing mechanisms with a more consistent network view, these models contribute to enhanced system robustness amid dynamic link conditions.

Satellite routing based on clustering. Unlike clustering in ad-hoc networks based on traffic or mobility patterns [15, 27], or static centralized clustering in satellite networks [31, 34], BlockFLEX leverages the intrinsic mesh topology of LSNs. It forms regular topological abstractions among adjacent satellites without actively steering ISL establishment. A distributed mechanism dynamically adapts block boundaries and topology in response to congestion or failures, preserving spatiotemporal adjacency where feasible. The primary novelty of BlockFLEX, compared to these systems, lies in its ability to simultaneously achieve routing efficiency and network resiliency in a fully distributed manner (§5.3), while its hierarchical addressing architecture ensures seamless interoperability with terrestrial networks (§5.1).

9 Discussion

Potential Enhancements in block evolution. One promising direction is to integrate reinforcement learning techniques. For example, abstracting block as agent, using the surrounding network information as the environment data, and selecting the optimal evolutionary actions based on their own states, instead of being triggered by ISL failure and congestion only, to achieve stronger survivability.

Trigger event of mode-switching. The stateful-stateless forwarding mode switching in our paper is to update all PFS and SFQ uniformly at a fixed time interval (100 sec). In fact, by choosing a suitable update mechanism, the routing performance can be better met while having lower overhead.

BlockFLEX for multi-shell satellite networks. As discussed in §5.1, BlockFLEX employs Earth-Centered Inertial (ECI) coordinate-based 3D addressing, which inherently supports

¹Starlink uses a centralized controller with 15s partial reconvergence for limited ISL traffic after G1.5 [53].

routing across multi-shell satellite constellations [10,33]. The inter-shell ISLs can be optimally coordinated through the wider view of self-adaptive block in DABNet architecture.

10 Conclusion

We have presented the design and implementation of BlockFLEX, a novel adaptive survivable architecture with hierarchical routing for LEO satellite networks, addressing the critical challenges posed by the volatile environment of LEO satellite networks. BlockFlex enhancing the survivability of underlay network by organizing multiple neighboring satellites into autonomous domains. Its also employ a hierarchical routing scheme, which combines convergence-free geographic routing between blocks and convergence-isolated routing within domains, minimizing routing overhead and improving overall resilience. Our evaluation demonstrates that BlockFLEX significantly improves network survivability, routing resiliency, and efficiency, even under critical failure conditions. This work provides a new direction for the design of resilient and efficient LEO satellite networks, paving the way for future advancements in space-based communication systems.

Availability

To facilitate double-blind review, all source code and data have been anonymized and are temporarily available at <https://github.com/wxton123/BlockFLEX>. The full, non-anonymized resources will be permanently archived upon acceptance.

References

[1] Konstantin Andreev and Harald Räcke. Balanced graph partitioning. In *Proceedings of the sixteenth annual ACM symposium on Parallelism in algorithms and architectures*, pages 120–124, 2004.

[2] LLC Application of Kuiper Systems. *Kuiper NGSO constellation FCC filing SAT-LOA-20190704-00057.* <http://licensing.fcc.gov/myibfs/forwardtopublicabaction.do?filenumber=SATLOA2019070400057>.

[3] Maciej Besta, Jens Domke, Marcel Schneider, Marek Konieczny, Salvatore Di Girolamo, Timo Schneider, Ankit Singla, and Torsten Hoefer. High-performance routing with multipathing and path diversity in ethernet and hpc networks. *IEEE Transactions on Parallel and Distributed Systems*, 32(4):943–959, 2020.

[4] Debopam Bhattacherjee and Ankit Singla. Network topology design at 27,000 km/hour. In *Proceedings of the 15th International Conference on Emerging Networking Experiments And Technologies*, 2019.

[5] Aydin Buluç, Henning Meyerhenke, Ilya Safro, Peter Sanders, and Christian Schulz. *Recent advances in graph partitioning*. Springer, 2016.

[6] Telesat Canada. *SAT-MPL-20200526-00053.* <http://licensing.fcc.gov/myibfs/forwardtopublicabaction.do?filenumber=SATMPL2020052600053>.

[7] Qiuwen Chen, Kechen Zheng, Feng Ouyang, Xiaoying Gan, Youyun Xu, and Xiaohua Tian. A shortest path routing algorithm based on virtual coordinate in nels. In *2016 8th International Conference on Wireless Communications & Signal Processing (WCSP)*, pages 1–5. IEEE, 2016.

[8] Quan Chen, Jianming Guo, Lei Yang, Xianfeng Liu, and Xiaoqian Chen. Topology virtualization and dynamics shielding method for leo satellite networks. *IEEE Communications Letters*, 24(2):433–437, 2019.

[9] Ltd. China Satellite Communications Group Co. Chinasat communication satellites. <http://www.chinasatcom.com/>, 2025. Accessed: 2025-06-01.

[10] Yi Ching Chou, Xiaoqiang Ma, Feng Wang, Sami Ma, Sen Hung Wong, and Jiangchuan Liu. Towards sustainable multi-tier space networking for leo satellite constellations. In *2022 IEEE/ACM 30th International Symposium on Quality of Service (IWQoS)*, pages 1–11. IEEE, 2022.

[11] David D Clark. *Designing an internet*. MIT Press, 2018.

[12] R Coltun, Dennis Ferguson, John Moy, and Acee Lindenm. Rfc 5340: Ospf for ipv6, 2008.

[13] Federal Communications Commision. *FCC Grants OneWeb US Access for Broadband Satellite Constellation.* <https://docs.fcc.gov/public/attachments/DOC-345467A1.pdf>, 2017.

[14] Thomas H Cormen, Charles E Leiserson, Ronald L Rivest, and Clifford Stein. *Introduction to algorithms*. MIT press, 2009.

[15] Ha Dang and Hongyi Wu. Clustering and cluster-based routing protocol for delay-tolerant mobile networks. *IEEE Transactions on Wireless Communications*, 9(6):1874–1881, 2010.

[16] Samson Vineeth Kumar Eguri, Arockia Bazil Raj A, and Nishant Sharma. Survey on acquisition, tracking and pointing (atp) systems and beam profile correction techniques in fso communication systems. *Journal of Optical Communications*, 45(4):881–904, 2024.

[17] Guojie Fan, Hewu Li, Jun Liu, Zeqi Lai, Wu Qian, Lu Lu, and Zheng Shaowen. User-driven flexible and effective link connection design for mega-constellation satellite networks. In *2023 International Wireless Communications and Mobile Computing (IWCMC)*, pages 793–799. IEEE, 2023.

[18] Daniel Fischer, David Basin, Knut Eckstein, and Thomas Engel. Predictable mobile routing for spacecraft networks. *IEEE Transactions on Mobile Computing*, 12(6):1174–1187, 2012.

[19] Aric Hagberg, Pieter J Swart, and Daniel A Schult. Exploring network structure, dynamics, and function using networkx. Technical report, Los Alamos National Laboratory (LANL), Los Alamos, NM (United States), 2008.

[20] Thomas R Henderson and Randy H Katz. On distributed, geographic-based packet routing for leo satellite networks. In *Globecom'00-IEEE.*, volume 2, pages 1119–1123. IEEE, 2000.

[21] ITU. Measuring digital development: Facts and figures 2022. ITU Publications, 2022. Accessed: [Access Date].

[22] Elliott D Kaplan and Christopher Hegarty. *Understanding GPS/GNSS: principles and applications*. Artech house, 2017.

[23] Simon Kassing, Debopam Bhattacherjee, André Baptista Águas, Jens Eirik Saethre, and Ankit Singla. Exploring the "internet from space" with hypatia. In *Proceedings of the ACM Internet Measurement Conference*, pages 214–229, 2020.

[24] Yagiz Kaymak, Roberto Rojas-Cessa, Jianghua Feng, Nirwan Ansari, MengChu Zhou, and Tairan Zhang. A survey on acquisition, tracking, and pointing mechanisms for mobile free-space optical communications. *IEEE communications surveys & tutorials*, 20(2):1104–1123, 2018.

[25] Alexander Kedrowitsch, Jonathan Black, and Daphne Yao. Resilient routing for low earth orbit mega-constellation networks. *Proceedings 2024 Workshop on Security of Space and Satellite Systems*, 2024.

[26] Ömer Korçak and Fatih Alagöz. Virtual topology dynamics and handover mechanisms in earth-fixed leo satellite systems. *Computer networks*, 53(9):1497–1511, 2009.

[27] Prasad Krishna, Nitin H Vaidya, Mainak Chatterjee, and Dhiraj K Pradhan. A cluster-based approach for routing in dynamic networks. *ACM SIGCOMM computer communication review*, 27(2):49–64, 1997.

[28] Zeqi Lai, Hewu Li, Yikun Wang, Qian Wu, Yangtao Deng, Jun Liu, Yuanjie Li, and Jianping Wu. Achieving resilient and performance-guaranteed routing in space-terrestrial integrated networks. In *IEEE INFOCOM 2023-IEEE Conference on Computer Communications*, pages 1–10. IEEE, 2023.

[29] Zeqi Lai, Qian Wu, Hewu Li, Mingyang Lv, and Jianping Wu. Orbitcast: Exploiting mega-constellations for low-latency earth observation. In *2021 IEEE 29th International Conference on Network Protocols (ICNP)*, pages 1–12. IEEE, 2021.

[30] P Lapukhov and A Premji. Rfc 7938: Use of bgp for routing in large-scale data centers, 2016.

[31] Rui Li, Jiaxin Zhang, Shuang Zheng, Kaiwei Wang, Peng Wang, and Xing Zhang. Leo mega-constellations routing algorithm based on area segmentation. In *2023 IEEE Wireless Communications and Networking Conference (WCNC)*, pages 1–6. IEEE, 2023.

[32] Yuanjie Li, Hewu Li, Wei Liu, Lixin Liu, Yimei Chen, Jianping Wu, Qian Wu, Jun Liu, and Zeqi Lai. A case for stateless mobile core network functions in space. In *Proceedings of the ACM SIGCOMM 2022 Conference*, pages 298–313, 2022.

[33] Yuanjie Li, Lixin Liu, Hewu Li, Wei Liu, Yimei Chen, Wei Zhao, Jianping Wu, Qian Wu, Jun Liu, and Zeqi Lai. Stable hierarchical routing for operational leo networks. In *Proceedings of the 30th Annual International Conference on Mobile Computing and Networking*, pages 296–311, 2024.

[34] Jiang Liu, Xinyuan Zhang, Ran Zhang, Tao Huang, and F Richard Yu. Reliable and low-overhead clustering in leo small satellite networks. *IEEE Internet of Things Journal*, 9(16):14844–14856, 2021.

[35] Lixin Liu, Hewu Li, Yuanjie Li, Zeqi Lai, Yangtao Deng, Yimei Chen, Wei Liu, and Qian Wu. Geographic low-earth-orbit networking without qos bottlenecks from infrastructure mobility. In *2022 IEEE/ACM 30th International Symposium on Quality of Service (IWQoS)*, pages 1–10. IEEE, 2022.

[36] Wenhao Liu, Jiazhi Wu, Quanwei Lin, Handong Luo, Qi Zhang, Kun Qiu, Zhe Chen, and Yue Gao. Efficient satellite-ground interconnection design for low-orbit mega-constellation topology. *IEEE Transactions on Mobile Computing*, 2024.

[37] Yong Lu, Fuchun Sun, and Youjian Zhao. Virtual topology for leo satellite networks based on earth-fixed footprint mode. *IEEE communications letters*, 17(2):357–360, 2013.

[38] Micah Maidenberg. SpaceX's Starlink nears cash-flow break-even. *The Wall Street Journal*, February 2023. Early announcement by SpaceX COO Gwynne Shotwell on profitability targets.

[39] Bomin Mao, Xueming Zhou, Jiajia Liu, and Nei Kato. On an intelligent hierarchical routing strategy for ultra-dense free space optical low earth orbit satellite networks. *IEEE Journal on Selected Areas in Communications*, 2024.

[40] Paul V Mockapetris. Rfc1034: Domain names-concepts and facilities, 1987.

[41] Julio C Navas and Tomasz Imielinski. Geocast—geographic addressing and routing. In *Proceedings of the 3rd annual ACM/IEEE international conference on Mobile computing and networking*, pages 66–76, 1997.

[42] Nils Pachler, Inigo del Portillo, Edward F Crawley, and Bruce G Cameron. An updated comparison of four low earth orbit satellite constellation systems to provide global broadband. In *2021 IEEE International Conference on Communications Workshops (ICC Workshops)*, pages 1–7. IEEE, 2021.

[43] Tian Pan, Tao Huang, Xingchen Li, Yujie Chen, Wenhao Xue, and Yunjie Liu. Op SPF: Orbit prediction shortest path first routing for resilient leo satellite networks. In *ICC 2019-2019 IEEE International Conference on Communications (ICC)*, pages 1–6. IEEE, 2019.

[44] Charles Perkins, Elizabeth Belding-Royer, and Samir Das. Rfc3561: Ad hoc on-demand distance vector (aodv) routing, 2003.

[45] Larry L Peterson and Bruce S Davie. *Computer networks: a systems approach*. Elsevier, 2007.

[46] Yakov Rekhter, Tony Li, and Susan Hares. A border gateway protocol 4 (bgp-4). Technical report, 2006.

[47] Idem Est Research. Country telecoms industry reports, March 2025.

[48] Reuters. SpaceX says plans to sell satellite laser links commercially, 2024. Accessed: 2024-03-19.

[49] Guido Rizzi and Matteo Luca Ruggiero. *Relativity in rotating frames: relativistic physics in rotating reference frames*. Springer, 2004.

[50] LLC Space Exploration Holdings. SpaceX ka-band ngso constellation fcc filing sat-loa-20161115-00118. <http://licensing.fcc.gov>.

[51] SpaceX. Starlink technology overview, 2024. Accessed: 2024-03-19.

[52] Chen Sun, Jun Bi, Haoxian Chen, Hongxin Hu, Zhilong Zheng, Shuyong Zhu, and Chenghui Wu. Sdpa: Toward a stateful data plane in software-defined networking. *IEEE/ACM Transactions on Networking*, 25(6):3294–3308, 2017.

[53] Hammas Bin Tanveer, Mike Puchol, Rachee Singh, Antonio Bianchi, and Rishab Nithyanand. Making sense of constellations: Methodologies for understanding Starlink's scheduling algorithms. In *Companion of the 19th International Conference on Emerging Networking EXperiments and Technologies*, pages 37–43, 2023.

[54] Christos Tsilopoulos, George Xylomenos, and Yannis Thomas. Reducing forwarding state in content-centric networks with semi-stateless forwarding. In *IEEE INFOCOM 2014-IEEE Conference on Computer Communications*, pages 2067–2075. IEEE, 2014.

[55] Hiroshi Tsunoda, Kohei Ohta, Nei Kato, and Yoshiaki Nemoto. Geographical and orbital information based mobility management to overcome last-hop ambiguity over ip/leo satellite networks. In *2006 IEEE International Conference on Communications*, 2006.

[56] Frank Uyeda, Marc Alvidrez, Erik Kline, Bryce Petruni, Brian Barritt, David Mandle, and Aswin Chandy Alexander. Sdn in the stratosphere: Loon's aerospace mesh network. In *Proceedings of the ACM SIGCOMM 2022 Conference*, pages 264–280, 2022.

[57] Arun Venkataramani, James F Kurose, Dipankar Raychaudhuri, Kiran Nagaraja, Morley Mao, and Suman Banerjee. Mobilityfirst: A mobility-centric and trustworthy internet architecture. *ACM SIGCOMM Computer Communication Review*, 44(3):74–80, 2014.

[58] Viasat. Viasat global satellite communications. <https://www.viasat.com/>, 2025. Accessed: 2025-06-01.

[59] Lloyd Wood. *Internetworking with satellite constellations*. University of Surrey (United Kingdom), 2001.

[60] Wang Xiangtong, Li Wei, Yang Menglong, Han Songchen, and Jiang Zhiyun. Enabling high-connectivity leo satellite networks via encountering inter-satellite links. In *IEEE Global Communications Conference (GLOBECOM)*, 2023.

[61] Wang Xiangtong, Han Xiaodong, Yang Menglong, Han Songchen, and Li Wei. Space networking kit: A novel simulation platform for emerging leo mega-constellations. In *IEEE International Conference on Communications*, 2024.

[62] Guoliang Xu, Yanyun Zhao, Yongyi Ran, Ruili Zhao, and Jiangtao Luo. Spatial location aided fully-distributed dynamic routing for large-scale leo satellite networks. *IEEE Communications Letters*, 2022.

[63] Yuanxi Yang, Weiguang Gao, Shuren Guo, Yue Mao, and Yufei Yang. Introduction to beidou-3 navigation satellite system. *Navigation*, 66(1):7–18, 2019.

[64] Yaoying Zhang, Qian Wu, Zeqi Lai, and Hewu Li. Enabling low-latency-capable satellite-ground topology for emerging leo satellite networks. In *IEEE INFOCOM 2022-IEEE Conference on Computer Communications*, pages 1329–1338. IEEE, 2022.

A The Maintaining Procedure of DABNet.

The complete DABNet maintaining procedure is shown in Algorithm.2. We define a function `BlockEvo()` to present the block evolution concurrently. Line 7 reconstructs the new block by preserving the maximum connected subgraph of the original block, while transitioning all remaining satellites to VAGRANT state; Line 8-10 releases the current Block entirely, with all associated satellites reverting to VAGRANT state; Line 11 indicates convergence to stable state, terminating the iteration; Line 14’s CQSBE constitutes the core evolutionary mechanism for DABNet maintaining.

Algorithm 2: DABNet Maintaining Framework

Input: Blocks set \mathcal{B}^t at time stamp t
Output: Block set \mathcal{B}^{t+1} at time stamp $t+1$

```

1 def BlockEvo(  $\mathcal{B}: \mathcal{B}^t$  )  $\rightarrow \mathcal{B}^{t+1}$ :
2    $\mathcal{B}^* \leftarrow \mathcal{B}^t$ ;
3   while true do
4     if STATE( $\mathcal{B}^*$ ) = DISCONN then
5        $\mathcal{B}' \leftarrow \mathcal{B}^* - \text{MaxSub}(\mathcal{B}^*)$ ; for  $s \in \mathcal{B}'$  do
6          $s.\text{STATE} \leftarrow \text{VAGRANT}$  ;
7          $\mathcal{B}^* \leftarrow \text{MaxSub}(\mathcal{B}^*)$ ;
8       else if STATE( $\mathcal{B}^*$ ) = LOWSIZE then
9         for  $s \in \mathcal{B}^*$  do  $s.\text{STATE} \leftarrow \text{VAGRANT}$ ;
10         $\mathcal{B}^* \leftarrow \emptyset$ ; break;
11       else if STATE( $\mathcal{B}^*$ ) = STABLE then
12         break; // stop evolution
13       else if STATE( $\mathcal{B}^*$ ) = USTABLE then
14          $\mathcal{B}^* \leftarrow \text{CQSBE}(\mathcal{B}^*)$ ;
15       end
16      $\mathcal{B}^{t+1} \leftarrow \mathcal{B}^*$ ; return  $\mathcal{B}^{t+1}$ 
17   end
18   for  $\mathcal{B}_k^t \in \mathcal{B}^t$  do
19     ThreadStart(BlockEvo
20     (  $\mathcal{B}_k^t$  )); // Multi-threads running
end

```

B Optimal Source Satellite Selection

Algorithm.3 shows the algorithm of OS3 (§5.4), at the beginning of routing, the GS maintains for each dataflow I_D a Source-satellite Priority Queue (SPQ) $Q[I_D]$. Then, one of the available satellites s_i is randomly selected for the active dataflow I_D , and if it is successful to delivery the data to the destination GS, the source GS g_{src} inserts (s_i, RTT) into the SPQ $Q[I_D]$ in ascending order by RTT (line 3). If the delivery is failed by selecting s_i as the source satellite, the GS will delete the corresponding data accordingly (line 9-11). After constructing Q and when no new satellites are available, the

Algorithm 3: Optimal Source Satellites Selection algorithm (OS3)

Input: datagram $D^t(I^t, D, r_{src}, r_{dst}, I_{src}, I_{dst})$ at time stamp t , A set of source satellites S_{src}^t , i.e., all feasible satellites connected to current GS.

Output: selected source satellite s_{src}

- 1 **Initialize:** $Q \leftarrow \emptyset$
// new connected satellites
- 2 **while** $s_i \in S_{src}^t - S_{src}^{t-1}$ **do**
- 3 $T[s_i] \leftarrow \text{Send}(s_i, D)$; // datagram delivery success
- 4 **if** $T[s_i]$ **then**
- 5 $Q[I_D].insert(s_i, T[s_i])$;
- 6 **return** s_i
- 7 **else continue;** // delivery failed
- 8 **end**
- 9 **while** $s_i \in S_{src}^{t-1} - S_{src}^t$ **do**
- 10 $Q[I_D].remove(s_i)$; // disconnected satellites
- 11 **end**
- 12 $(s_{src}, T[s_{src}]) \leftarrow Q[I_D].pop()$; $T[s_{src}] \leftarrow \text{Send}(s_{src}, D)$;
 $Q[I_D].update(s_{src}, T[s_{src}])$;
- 13 **return** s_{src}

ground station selects the satellite with the minimum RTT from Q^{I_D} as the source satellite for dataflow I_D (line 12).

C Algorithm Complexity Analysis

CQSBE. In the term of ϕ 's computation (Algorithm.1 line 3), it requires all-pairs shortest path (APSP) analysis within block \mathcal{B} . For a block containing $|\mathcal{V}_{\mathcal{B}}|$ nodes, the time complexity is $O(|\mathcal{V}_{\mathcal{B}}||\mathcal{E}_{\mathcal{B}}| + |\mathcal{V}_{\mathcal{B}}|^2 \log |\mathcal{V}_{\mathcal{B}}|)$ where $|\mathcal{V}_{\mathcal{B}}|, |\mathcal{E}_{\mathcal{B}}|$ are the number of satellites and links in block \mathcal{B} [14]. In the term of ψ 's computation, the complexity related to the block size $N_{\mathcal{B}}$ and number of adjacent VAGRANT satellites m , yielding $O(m \cdot N_{\mathcal{B}}^2)$. In the worst case (fully connected network), k scales linearly with network size $N_{\mathcal{B}}$. Thus, the complexity of the evolutionary process will at most not exceed that of $O(N_{\mathcal{B}}^3)$. Since $N_{\mathcal{B}}$ will generally be maintained at a small level (< 10 in all our evaluations) and the frequency of triggering network failure is not very high, each block evolutionary complexity will be maintained at a suitable level.

nBAS. nBAS mechanism can run purely distributed in Block-FLEX, and as the queue length n and the number of dataflow increase, the cost of maintaining the PFS in each unit will rise sharply. Considering the limited holding time of dataflow in highly dynamic satellite networks, the PFS maintained in each forwarding unit will also be dynamically emptied over time to reduce the resource consumption of the forwarding unit. Compared with the traditional convergence-free GEO

routing that calculates next-hop by Eq.8 - Eq.10 after ingressing each packet, the nBAS method is used only when the dataflow is first ingressing the current unit, and the PFS is constructed by calculating the matching degree ranking, and the forwarding in the future period is based on the PFS. The stack header of the PFS is matched, which further reduces the overhead caused by frequent locator computation (§5.1), and can bring great overhead savings at high throughput. The nBAS algorithm employs a DFS-like strategy to traverse the state space of candidate paths. Its time and space complexity depend on the network scale (number of nodes and edges) and the maximum search depth n . Through heuristic pruning and distributed computation, the actual complexity remains manageable, making it suitable for dynamic LSN environments.

OS3. When a ground station g_{src} has N active dataflows and M newly accessible satellites become available within a certain period, it requires $N \cdot M$ probing attempts, with results inserted into the maintained queues. This yields both time and space complexity of $O(NM)$. Although selecting only at the source satellite side cannot guarantee identification of the minimum-delay satellite-ground topology, this method can operate in a fully distributed manner within relatively low complexity bounds, making it practically significant for real-world implementations.

D Network Failure Model

In this work, we employ a network failure model to investigate network survivability. In LSNs, satellite failures can be considered as the unavailability of all attached ISLs; thus, network failures can be represented as sets of ISL failures. For any ISL, we define an availability function $Z_{e_i}(t)$ to indicate whether the ISL e_i is operational at time t . A straightforward failure model uses a periodic square wave to represent ISL availability, where the duty cycle, frequency, and phase can be preset to control failure duration, occurrence frequency, and temporal distribution. By applying randomly distributed phases across the availability functions $Z_{e_i}(t)$ of all ISLs, we simulate network-wide intermittent link failure scenarios, as is shown in Fig.16.

However, actual ISL failures rarely exhibit such regularity. A more realistic model correlates link instability with dynamic network conditions: ISL experiencing higher dynamics are more prone to interruptions, which is a recognized behavior in satellites equipped with optical ISL and ATP [16] (Acquisition, Tracking, and Pointing) systems. More complex failure models could also incorporate factors such as solar illumination, though such extensions are beyond the scope of this work.

E Acronyms in This Work

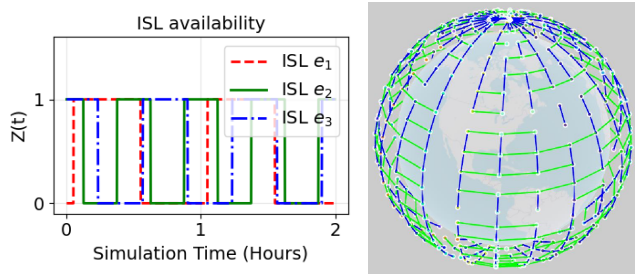


Figure 16: ISL availability function (left) and the LSN (OneWeb) with intermittent failure ISLs.

DABNet	Dynamic Adaptive Block Network
DABR	DABNet Routing
CQSBE	Connection Quality Score Block Evolution
SLP	Survivable LSN Partitioning
FU	Forwarding Unit (Blocks or vagrant satellites)
IUL	Inter Unit Link
MDV	Minimum Deviation Verte
CTV	Closer to Target Verte
MTA	Minimum Triangle Area
GNS	Global Name Server
GNSS	Global-Navigation-Satellite-System
ECI	Earth-Centered Inertia
nBAS	n-step Backward Acknowledgment Signalling
PFS	Protection Forwarding Stack
SPQ	Source satellite Priority Queue
FIB	Forwarding Information Base
GEO	Geostationary Earth Orbit
LEO	Low Earth Orbit
LSN	LEO Satellite Networks
GS	Ground Station
ISL	Inter Satellite Link